A Novel Tandem of Thermal Desorption Carbon Analyzer and Off-Axis Integrated Cavity Output Spectroscopy for Aerosol Stable Carbon Isotope Ratio Measurement

Daya S. Kaul[1], Zhi Ning[1,2]*, Dane Westerdahl[2], Xijie Yin[3], Robert A. Cary[4]

[1] *School of Energy and Environment, City University of Hong Kong, Hong Kong*
[2] *Guy Carpenter Asia-Pacific Climate Impact Centre, City University of Hong Kong, Hong Kong*
[3] *Laboratory of Ocean and Coast Geology, Third Institute of Oceanography, State Oceanic Administration, Xiamen, China*
[4] *Sunset Laboratory Inc., Tigard, OR, USA*

ABSTRACT

A novel approach for measurement of stable carbon isotopic ratio of atmospheric aerosols was developed by tandem operation of two instruments: a Sunset Organic Carbon-Elemental Carbon (OC-EC) analyzer and an online Carbon Dioxide Stable Isotope Analyzer (LGR, CCIA-36d). Sensitivity, accuracy and measurement uncertainty of the CCIA was comprehensively investigated using the standard reference CO_2 gas with known concentration and isotopic ratio. Drift in CCIA measurement due to varying CO_2 and water vapor concentration was evaluated and a humidity stabilizer was designed and developed to control the water vapor concentration of exhaust gas flow from OC-EC prior to entering the CCIA. A Keeling approach was applied to separate the ratio in the samples from the mixture of PM sample-produced CO_2 and reference gas and we developed a protocol to derive the isotopic composition of the particle samples. A lithium carbonate standard (in powder form) from National Institute of Standards and Technology (NIST) was used to validate measurement of $\delta^{13}C$ ratios by CCIA. Offline measurement on ambient aerosol and diesel exhaust aerosols produced comparable results of isotopic ratio with literature values. This study demonstrates the utility of this tandem operation for carbon isotopic measurement of atmospheric particles with better than 1.0‰ precision as a cost-effective alternative of conventional Isotopic Ratio Mass Spectrometer (IR-MS).

Keywords: OC-EC; OA-ICOS; Keeling curve; Stable isotopic ratio; Organic aerosol.

INTRODUCTION

Carbonaceous content of atmospheric particulate matter (PM) plays a crucial role in human health, air quality and climate change (Ramanathan *et al.*, 2005; Tie *et al.*, 2009; Wang *et al.*, 2014). Carbonaceous fraction accounts for ~20–90% of particulate mass depending upon geographical location and predominance of sources of the region (Zhang *et al.*, 2007; Jimenez *et al.*, 2009). Primary contributors to this fraction are vehicular exhaust emissions, biomass burning, coal power plants, industrial emissions etc. (Gilardoni *et al.*, 2011; Cao *et al.*, 2013). Carbonaceous aerosol is also produced through secondary processes such as photochemical oxidation reactions of precursor volatile organic compounds emitted from various sources (Jimenez *et al.*, 2009). A considerable portion of this carbon is contributed by toxic

organic compounds, many Poly Aromatic Hydrocarbons (PAHs), semi-Volatile Organic Carbon (semi-VOC) and oxygenated organics etc. (Adler *et al.*, 2011; Lammel *et al.*, 2011; Ehn *et al.*, 2014). These carbonaceous components interact directly or indirectly with incoming solar radiation and alter the radiation budget of the planet, weather and the climate (Ramanathan *et al.*, 2005). Thus, it is utmost important to understand the sources of atmospheric carbon-containing PM. The techniques widely used for this purpose are source apportionment, chemical mass balance-molecular marker approach etc. (Ke *et al.*, 2008; Heo *et al.*, 2013). These approaches require detailed chemical composition of atmospheric aerosols, usually measured using numerous advanced analytical instruments such as Inductively Coupled Plasma-Mass Spectrometry (ICP-MS), Gas Chromatography-Mass Spectrometry (GC-MS), High Resolution-Time of Flight-Mass Spectrometer (HR-ToF-AMS) to quantify metal, PAHs, semi-VOCs concentrations and tracer compounds (Ke *et al.*, 2008; Xu *et al.*, 2009; Alier *et al.*, 2013; Crippa *et al.*, 2014). In addition, numerous samples are required for performing source apportionment as technique is often based on statistical approach. Recently, isotopic ratio

---

* Corresponding author.
 Tel.: +852-3442-4620
 E-mail address: zhining@cityu.edu.hk

measurement of PM chemical components has been used as new and potentially powerful tool for source identification and apportionment (Fisseha *et al.*, 2006; Miyazaki *et al.*, 2012; Irei *et al.*, 2014; Masalaite *et al.*, 2015). Specifically, a few studies have used both stable and radioactive carbon isotope to perform source apportionment of carbonaceous aerosols (Ceburnis *et al.*, 2011; Kirillova *et al.*, 2014; Liu *et al.*, 2014; Zhang *et al.*, 2014).

One widely used instrument for measuring gas phase carbon isotopes is based on dual and continuous Isotopic Ratio Mass Spectroscopy (IRMS) which measure carbon isotopes in CO_2. These techniques rely on ion mass spectra measurement which requires large instrumental components and operation in a controlled environment making them difficult to include in field deployment. Improvements have been made that partially deal with these problems, and a new technique, namely Off Axis-Integrated Cavity Output Spectroscopy (OA-ICOS) that measures CO_2 stable isotope ratio online was recently developed. Although the technique provides lower precision in the measurements compared to IRMS, it does not require purification of sample gas as in IRMS, and sample is analyzed continuously compared to batch mode operation of IRMS. In addition, it provides measurements at high temporal resolution (as high as 1 Hz) and may be deployed in the field. It was primarily developed for monitoring the isotopic components of atmospheric CO_2 but offers application to varying sources and ranges of CO_2 from ambient atmosphere to volcanic origin. Neither of these techniques (OA-ICOS and IRMS) can be directly applied for carbon isotope measurement of aerosol samples. Some investigators have attempted to oxidize aerosol carbon content into equivalent CO_2, followed by isolation and injection into IRMS for isotope measurement (Cao *et al.*, 2011). Efforts have also been made to link a thermal-based carbon measuring instrument and a GC with an IRMS for this purpose (Huang *et al.*, 2006; Kawashima and Haneishi, 2012).

However, these attempts have been often limited by the complex operation of cumbersome advanced instruments and long sample pretreatment processes (Huang *et al.*, 2006; Kawashima and Haneishi, 2012). In this work we developed and validated a novel technique for stable carbon isotope measurement of OC and EC fractions in PM samples by combining two techniques namely TD carbon analysis (Sunset OC-EC Analyzer) and OA-ICOS (LGR, CCIA-36d). The method demonstrates acceptable precision to identify PM samples from different sources.

EXPERIMENTAL METHODOLOGY

In this study, we first evaluated the performance of an Off Axis-Integrated Cavity Output Spectroscopy (OA-ICOS) (Herriott *et al.*, 1964; Herriott and Schulte, 1965) based carbon dioxide online isotope analyzer and a thermal desorption based organic carbon/elemental carbon online analyzer, followed by an investigation of the feasibility of the tandem operation of the two instruments where the CO_2 exhausted by the Sunset Labs machine could be evaluated in the CCIA. Detailed laboratory evaluation and NIST

standard sample validation are also described and presented.

Stability and Sensitivity of CCIA

A Carbon Dioxide Isotope Analyzer (CCIA-36d, LGR, Los Gatos Research) measuring stable isotopic ratio ($\delta\,^{13}C$) of two stable isotopes of carbon (^{12}C and ^{13}C) in CO_2 was first evaluated. This instrument provides continuous measurement at 1 Hz with dynamic concentration range from ~300 to 25000 ppm. The manufacturer specifies that CCIA provides precision of ~0.15‰ for $\delta\,^{13}C$, ~3 ppm for ^{12}C and ~50 ppb for ^{13}C. Ambient air is drawn at 0.4 litre per minute (lpm) (flow rates could also be varied) through the cavity cell which is maintained at constant temperature and pressure. The laser is fired at very high frequency through the sample volume in the cavity and incident light bounces between the mirrors on both ends producing a long path length (diagram shown in supplementary information, Fig. S1). The isotopic ratio is estimated using ^{12}C and ^{13}C concentration against Pee Dee Belemnite (PDB) as described elsewhere (Guillon and Agrinier, 2012).

The accuracy and sensitivity of the CCIA measurement was analyzed on a short and long time series based measurement data (~30 min and 10 days, respectively). For the purpose, standard reference gas (calibrated with IRMS, details in the supplementary information, Section S1 and Fig. S2) of known CO_2 concentration (408 ± 4 ppm) and isotopic ratio ($\delta\,^{13}C$) (–17.8 ± 0.2‰) was injected into CCIA for short duration (~30 min). For long terms drift evaluation (stability), CO_2 from the 408 ppm cylinder was injected into CCIA for 10 minutes every 3 hours continuously for 10 days; the CCIA sampled ambient air between the standard CO_2 injections during the long term measurement period. Allen variance on CO_2 concentration and isotope $\delta\,^{13}C$ ratio data was investigated to assess instrument performance.

The CCIA measurement of isotopic ratios has been known for its CO_2 concentration dependence (Guillon and Agrinier, 2012); thus, sample specific correction curves to compensate for non-linear response were produced for correction. A dilution system (Lotun Science, S102-D) was used to produce different concentration of CO_2 (from 400 to 1300 ppm) from the reference gas (52000 ppm cylinder; $\delta\,^{13}C$ = –20.8 ±0.2‰) by diluting it with zero air. The CO_2 gas at different concentrations (400, 500, 600, 700, 800, 900, 1000, 1100, 1200, 1300 ppm) was injected in sequence into CCIA and each step was kept for 5 min. The initial 3 min data of every 5 mins was discarded to assure stable pressure condition was achieved between the steps. Such measurements were carried out prior to every solid sample analysis by OC-EC analyzer and the data acquired were used to derive sample specific correction curve between CO_2 concentration and isotopic ratio. The non-linear response was estimated as difference in ratio between that measured by the CCIA and reference value of standard gas (–20.8‰).

Water vapor in the sample gas, if not treated, may produce systematic error in isotopic measurement according to the manufacturer and this effect has been documented elsewhere (Gianfrani *et al.*, 1997). Sensitivity of ~–0.2 to –0.4‰ per 1000 ppm water vapor has been reported by Gianfrani *et al.* (1997) and Gilardoni *et al.* (2011). Two kinds of experiments

were performed to deal with these problems; 1) investigation of drift due to varying water vapor concentration and 2) a setup to control and stabilize water vapor during TD-OA-ICOS tandem operation. We designed a humidity stabilizer with the gas sample passing through a Nafion tube coil in the headspace of a glass flask with saturated salt solution in slurry form in the bottom of the flask. Water vapor moves into or out of the Nafion tube depending upon the partial water vapor pressure inside the Nafion tube (Wilson and Birks, 2006). Drift in CCIA ratio measurement was investigated using the Nafion tube and aqueous solution of four different salts (CH_3COOK, $MgCl_2$, $Mg(NO_3)_2$ and K_2SO_4) were used to produce four different values of water vapor concentration (~490, 880, 1800, 7700 ppm, respectively) in the CO_2 reference gas flow (varying concentration: 400, 500, 600, 700, 800, 1000, 1500, 2000, 2500, 3000 ppm) for the purpose (in supplementary information, Figs. S3–S4). The observation of drift due to varying water vapor vs. dry reference CO_2 gas was derived using four data points acquired using the said salts. Second, while running OC-EC and CCIA in tandem (refer section 2.3 for more details) for actual measurement, a slurry of salt (CH_3COOK), as described before, with Nafion tube was used to dry the input gas flow (Fig 1).

Organic Carbon-Elemental Carbon (OC-EC) CO_2 Output Profile

The OC-EC analyzer operates by thermal desorption of solid phase carbon and oxidation into equivalent CO_2 gas to quantify the carbon content. A typical output profile from OC-EC analyzer is shown in Fig. S5 (in supplementary information) with oven temperature, pressure, laser signal and CO_2 concentration during analysis. It can be run in both offline mode (sample is injected manually for OC and EC measurement) and semi-continuous mode (instrument collects ambient aerosol on a quartz filter for specified duration and then analyzes for its OC and EC content). The temperature inside the oven is ramped up in steps for thermal desorption of aerosol carbon (Fig. S5). The pyrolyzed compounds are oxidized with manganese dioxide into equivalent CO_2 which is quantified using a built-in non-dispersive infrared (NDIR) sensor. The CO_2 concentration measured by NDIR is shown in Fig. S5 (1st CO_2 peak in Fig. S5). A similar second temperature ramp is applied to quantify the EC which is also oxidized to equivalent CO_2 (2nd CO_2 peak in Fig. S5). OC and EC are automatically determined by dividing their peak areas by internal calibration peak of methane gas for each sample (Last CO_2 peak in Fig. S5).

OC and EC split time is estimated by monitoring the laser transmittance to reach the same starting level. EC generated from OC charring is automatically corrected using laser transmittance. More details on charring and split time can be found elsewhere (Birch and Cary, 1996; Chow *et al.*, 2001). An external calibration with the known carbon content (sucrose) was performed in the beginning of the experiment to ensure accuracy in the measurement. A total of five such standards with different concentrations (2, 6, 12, 14, 20 mg L^{-1}) were prepared. These standards were impregnated onto pre-conditioned quartz filters (baked at 800°C prior to analysis) for their OC-EC analysis to perform multipoint calibration of OC-EC analyzer. Correlation between measured and injected carbon was 1:1 with R^2 ~0.99. All the measurements by OC-EC analyzer were performed following NIOSH 5040 protocol (Birch and Cary, 1996).

Tandem Setup of OC-EC and CCIA Analyzers

The schematic of the tandem setup of OC-EC and CCIA analyzers is depicted in Fig 1. CO_2 from the OC-EC instrument exits at ~67 mlpm constant flow during analysis whereas CCIA required a flow rate of 400 mlpm. Thus, 600 ppm concentration of CO_2 was mixed with the exhaust stream from OC-EC analyzer to supply the required flow rate and maintain a baseline (background) CO_2 concentration prior to entering CCIA. The humidity stabilizer controls the concentration of water vapor to around 500 ppm before it enters into CCIA, as mentioned before. More details on water vapor and its influence on the CCIA measurement are discussed in Section 3.1.3.

CO_2 measured by NDIR of OC-EC analyzer and OA-ICOS of CCIA were compared for different samples to ensure consistency and accuracy of measurements by these detectors
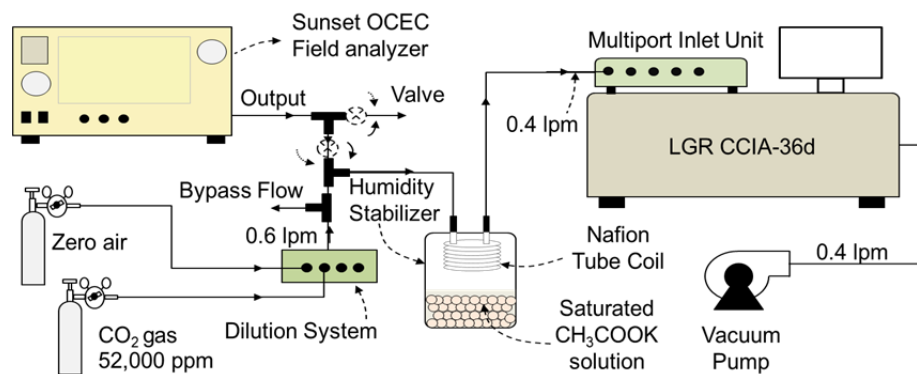

Fig. 1. Tandem setup Organic Carbon-Elemental Carbon (OC-EC) analyzer and Carbon Dioxide Stable Isotope Analyzer (CCIA). When top valve is opened, bottom is closed and vice versa. Top valve is opened to release the water vapor from OC-EC instrument into ambient preventing it from entering into CCIA during drying and purging process of the analysis. Top valve is closed and bottom is opened when carbon analysis starts.

in tandem operation. Sucrose samples and NIST standards of Lithium Carbonate (Li_2CO_3) (NIST SRM-8545), of multiple concentrations, were applied for this purpose.

Offline Sample Preparation

Three different types of samples were used for performance evaluation of the OCEC-CCIA tandem setup for derivation of isotopic ratios. (1) Ambient aerosols samples were collected on quartz filters using Personal Cascade Impactor Sampler (PCIS) (SKC Inc.; cut off size = 2.5 μm; flow rate = 9 lpm) in roadside of busy streets in Hong Kong (10 samples) as part of public transport passenger exposure study (Yang *et al.*, 2014); (2) Diesel engine exhaust PM samples were collected from the engine dynamometer facility at Hong Kong Polytechnic University as part of diesel exhaust PM characterization study (Zhou *et al.*, 2014; Man *et al.*, 2015). The exhaust particles were collected on quartz filter (10 samples) using stainless steel filter holders at 10 lpm. All the quartz filters used for sample collection were prebaked at 800°C prior to sampling for 5 hours to remove background carbon content on the filter; (3) A total of 5 NIST standard samples of Li_2CO_3 ($\delta^{13}C$ = –46.6‰, LSVEC: Lithium and Carbon isotope in Lithium Carbonate) with different masses were used to validate the results of OCEC-CCIA tandem measurements.

RESULTS AND DISCUSSIONS

Characteristic of CCIA and its Performance
Short and Long Term Performance of CCIA Measurement

Figs. 2(a) and 2(b) show CO_2 concentration and $\delta^{13}C$ ratio of reference gas (CO_2 = 408 ppm; $\delta^{13}C$ = –17.8 ± 0.2‰) measured by CCIA for 30 min duration. Allen deviation is used to characterize the stability in measurement. It provides the expected standard deviation of the measurement for certain averaging time. It characterizes the precision of the measurement and timescale of instrumental drift. The drift puts a threshold on integrating time to remove noise in the measurement which occurs when Allan curve turns up (Werle *et al.*, 1993; Croize *et al.*, 2010; Werle, 2011; Guillon and Agrinier, 2012) indicating increase in variance. For example, Fig. 2(c) indicates that noise could be reduced by taking below 120 s average but above 120 s average, the noise will increase because Allen curve has turned up. It is claimed by the manufacturer to provide better than 0.25‰ precision on 60 s integrated time base. Allan deviation of a 30-min measurement, shown in Fig. 2(c) indicated that averaging time of 5 s and 60 s will result in relatively low noise and variance in the measurement. Averaging over 60 s yields ~0.15 and 0.05 Allan deviations for $\delta^{13}C$ and CO_2 concentration, respectively, while 5 s averaging time produces
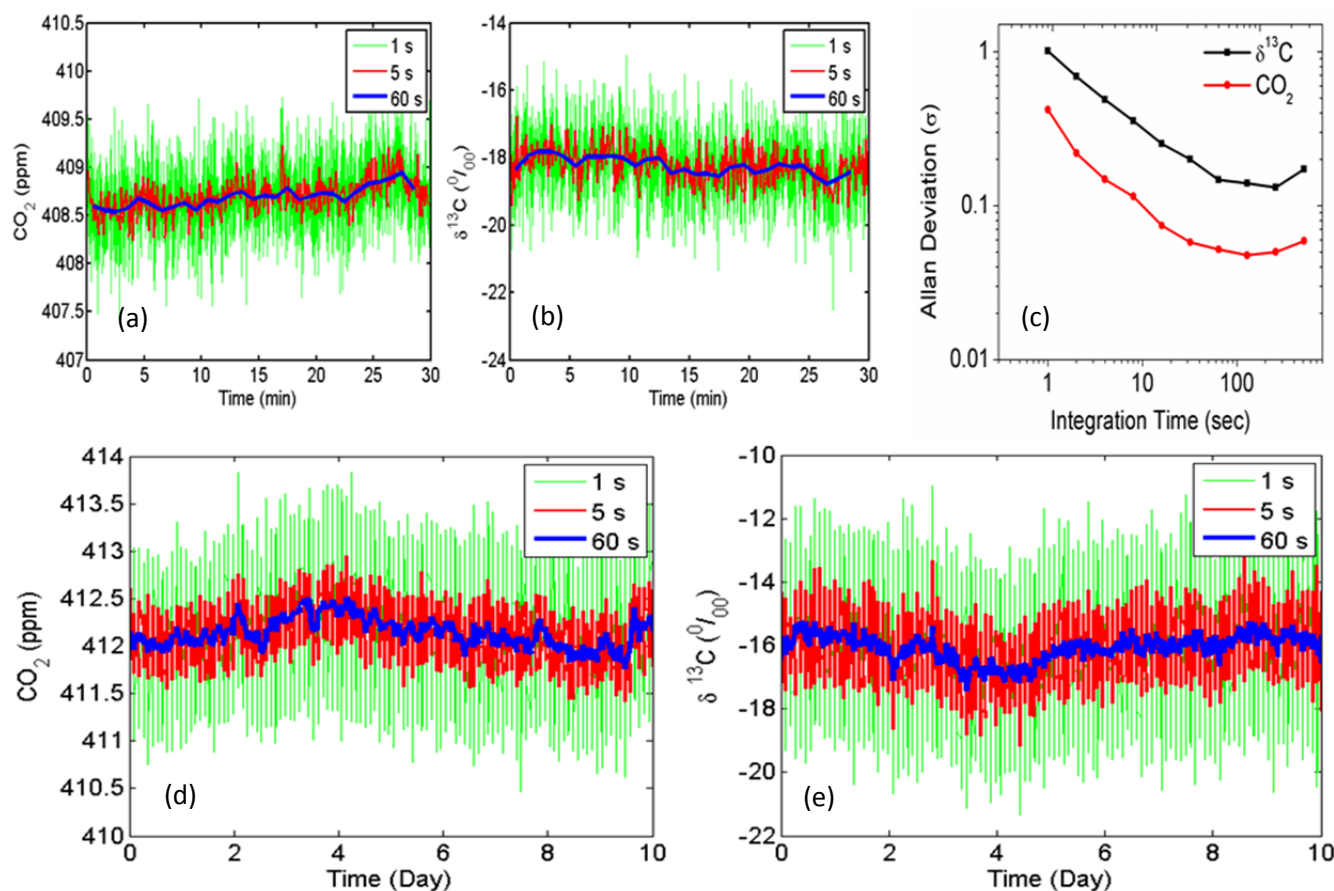

Fig. 2. CCIA measurement performance evaluation: a). CO_2 concentration from a 30-min measurement; b). $\delta^{13}C$ ratio from a 30-min measurement; c). Allan deviation from a 30-min measurement; d) CO_2 concentration from a 10-day continuous measurement; and e). $\delta^{13}C$ ratio from a 10-day continuous measurement.

corresponding Allan deviations of ~0.40 and 0.150 (Fig. 2(c)).

Figs. 2(d) and 2(e) show the long term measurement uncertainty of CO_2 concentration and $\delta^{13}C$ ratio from the 10-day test. The standard deviation of CO_2 and $\delta^{13}C$ measurements for 1 s, 5 s and 60 s were 0.49, 0.22, 0.16 ppm and 1.3, 0.74, 0.46‰, respectively, for the entire 10 days measurement. There is no systematical drift observed from the long duration test for both CO_2 concentration and $\delta^{13}C$ ratio measurements (Figs. 2(d) and 2(e)). However, comparing short (Figs. 2(a) and 2(b)) and long term test results (Figs. 2(d) and 2(e)), it is worth noting that CO_2 concentration was at reference value of ~408 ppm at short term test, while it was ~412 ppm at long term test after the CCIA experienced a few restarts (Figs. 2(a) vs. 2(d)); and similar discrepancy was found for $\delta^{13}C$ with ~−16.0‰ and ~−18.0‰ for short and long term tests, respectively (Figs. 2(b) vs. 2(e)). Thus, CCIA data need to be corrected from reference gas each time after a cold start and during the long term measurement as recommended by the manufacturer.

Drift in CO_2 and Isotopic Ratio Measurement of CCIA

Fig. 3 shows the relation between the CO_2 concentration and corresponding drift in isotopic ratio and CO_2. Concentration dependent drift of $\delta^{13}C$ has been reported as a main source of errors in CCIA measurement (Guillon and Agrinier, 2012). Since concentrations of CO_2 from OC-EC analyzer depends upon carbon loading of samples, there may exist a wide range of CO_2 levels (range ~0–20000 ppm) and it is vital to develop a correction curve covering typical concentration range of measured CO_2, which is the mixture of background CO_2 gas and exhaust of OC-EC analyzer as explained in Section 2.3. Finding a universal mathematical model to fit a full range of concentration is often difficult and an improper fit would not produce desired level of accuracy required in the current study. Thus, we limited the range of CO_2 concentration between ~400 to 1300 ppm to develop sample specific correction curve for the anticipated range (more details about selection of this range and error is described in supplementary section S2-II) for better accuracy. As shown in Fig. 3(b) (for a typical sample), the CCIA showed a non-linear drift in $\delta^{13}C$ ratio measurement

with varying CO_2 concentrations and trend is similar to that reported by Guillon and Agrinier (2012). Drift varies over time thus it is desirable to develop the correction curve prior to each sample analysis (or prior to 1–3 immediate analyses) to reduce the uncertainty of $\delta^{13}C$ ratio measurement.

Correction curve (Fig. 3(a)) is fitted with Eq. (1) (using Matlab least square curve fitting function: lsqcurvefit) to estimate drift and correct for the subsequent analyzed sample by OC-EC analyzer. The coefficients of the Eq. (1) are sample specific for better accuracy. A typical curve fitted and its residual (which is < 0.5‰) shown in Fig. 3 indicates that error in correction applied to the subsequent sample will be lower than 0.5‰. Thus, error due to application of correction will be considerably small and in acceptable range. We also observed slight drift in CO_2 of CCIA measurement (against the standard injected CO_2 concentration) (Fig. 3(b)). The same equation (Eq. (1)) was fitted to correct subsequent CO_2 measurement as well. The coefficients for this curve will also be sample specific but different than for ratio correction fit. A typical curve shown in Fig. 3(b) indicates acceptable residual (which is < 6.0 ppm). Such a small residual will incur almost negligible error in correcting real subsequent samples (More detail on error in supplementary section S2).

$$\delta^{13}C_{ccia} - \delta^{13}C_{ref} = C_1 + C_2 \times \left\{ \frac{[CO_2]}{C4} - e^{-[CO_2]/C3} \right\} \qquad (1)$$

where, $\delta^{13}C_{ccia}$ is $\delta^{13}C$ measured by CCIA and $\delta^{13}C_{ref}$ is $\delta^{13}C$ of reference gas in (‰); CO_2 concentration is in ppm.

Impact of Water Vapor on CCIA Isotopic Ratio Measurement

Preliminary investigation in CO_2 exiting from the OC-EC instrument showed variable amount of water vapor in different samples, either coming from thermal desorption of particle sample or from ambient air while injecting samples into the OC-EC analyzer. Water vapor concentration was negligible in reference gas cylinders and ~1,000–4,000 ppm in the exit gas flow of OC-EC analyzer. Such variation may

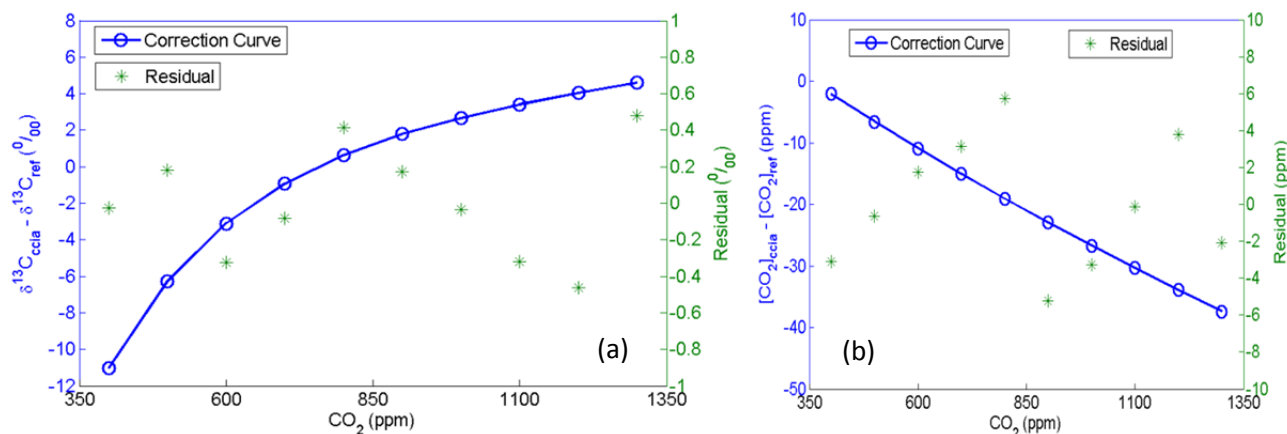**Fig. 3.** Drift in (a) $\delta^{13}C$ and (b) CO_2 measurement due to change in CO_2 concentration (measured against the reference value of the standard gas).

be a concern for CCIA measurement uncertainty and become a source of error. Thus, a stabilization of varying water vapor concentration for the input to CCIA was necessary. The drift depends on CO_2 and water vapor concentrations and becomes more prominent in high and low CO_2 concentration range (as shown in Fig. S4). This figure clearly indicates that if instrument is operated in middle CO_2 range and lower water vapor, drift in the measurement could become considerably small. While running the setup in the OC-EC-CCIA tandem mode, the Nafion tube set up with flask filled with single salt, CH_3COOK which can produce lowest possible humidity among the four salts (CH_3COOK, $MgCl_2$, $Mg(NO_3)_2$ and K_2SO_4 produced four different values of water vapor concentration ~490, 880, 1800, 7700 ppm, respectively) was placed before CCIA to dehumidify and stabilize water vapor concentration in the mixture of gases from OC-EC output and reference CO_2 cylinder (Fig 1). Each sample was dried and OC-EC instrument was purged prior to analysis. During filter drying and instrument purging, the exhaust gas mixture from OC-EC instrument was vented to the ambient air to prevent entry of any water vapor into CCIA. When the actual analysis started, exhaust of OC-EC was connected to CCIA using manual switch (Fig 1). With Nafion tube and single salt (CH_3COOK), water vapor was controlled to below ~500 ppm and thus uncertainty in the actual measurement was also within ~−0.15‰. The precision in the ratio measurement with water vapor control was ~0.15‰. It has to be noted that reference gas cylinders are devoid of water vapor, thus measurement for producing Figs. 2 and 3 would not be affected.

Comparison of CO_2 Measurement by CCIA and OC-EC Analyzers

The carbon content of samples is determined by integrating the CO_2 concentration in thermograph as measured from OC-EC analyzer. In order to ensure of the consistency of carbon measurement by OC-EC and CCIA tandem system, the CO_2 concentration from NDIR sensor of OC-EC analyzer and OA-ICOS detector of CCIA were determined separately and compared. Different types of samples (Sucrose and NIST standards) were analyzed in OC-EC instruments and produced CO_2 was injected into CCIA. Since, CO_2 output from OC-EC analyzer was mixed with CO_2 from the reference gas cylinder to maintain the required flow by CCIA, the height of peak and its width of CO_2 concentration measured by CCIA would vary (in supplementary, Fig. S6). Thus, to compare these detectors, the areas of CO_2 profile measured by OC-EC analyzer and CCIA (CO_2 measurement by CCIA were corrected for dilution by reference) were integrated (Fig. 4). A one to one correlation was observed (R^2 ~0.99) showing accurate and consistent carbon measurement across different platforms (Fig 4).

Carbon Isotopic Ratio Measurement

NIST standards (Lithium carbonate) of known $\delta^{13}C$ ratio were used as reference samples for the OC-EC and CCIA tandem performance evaluation. Flow in CCIA was maintained by injecting CO_2 from a reference gas cylinder (600 ppm) and OC-EC produced CO_2 was measured against a
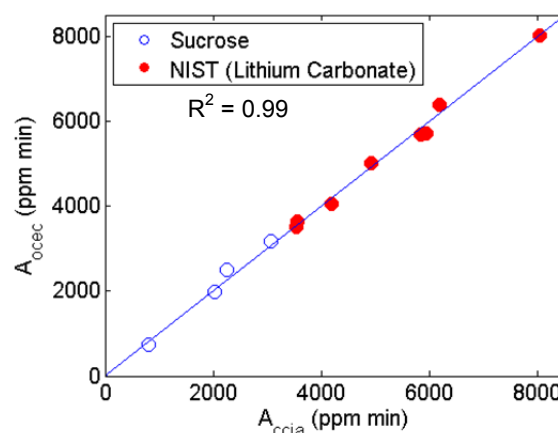

Fig. 4. Comparison of integrated CO_2 area (A) under OC profile of CCIA and OC-EC analyzer. To compare these detectors, the areas of CO_2 profile measured by OC-EC analyzer and CCIA (CO_2 measurement by CCIA were corrected for dilution by reference) were integrated. A one to one correlation (R^2 ~0.99) shows accurate and consistent carbon measurement across both platforms.

baseline of ~500 after dilution by He flow. CO_2 entering the CCIA was a mixture of reference CO_2 gas (cylinder) and that exiting the OC-EC analyzer. Water vapor was controlled as described above (Fig. 1) and correction developed for varying CO_2 (Eq. (1)) were applied to correct $\delta^{13}C$ and CO_2 measurement by CCIA. Correction curve for CO_2 drift was produced for every sample before the OC-EC analysis and the subsequent CCIA measurement for each sample were corrected by such sample specific individual correction curves. A Keeling approach (Pataki *et al.*, 2003) was adopted to separate the isotopic ratio of NIST standard values from the mixture of CO_2 produced from combustion of NIST standard and background value of the reference gas cylinder. In this approach, $\delta^{13}C$ added from OC-EC analyzer could be easily separated from the background $\delta^{13}C$ ratio of the reference cylinder by the following approach.

Total mixture concentration (C_m) of CO_2 is sum of CO_2 from the source (C_s) and background (C_b),

$$C_m = C_b + C_s \tag{2}$$

Conservation of mass produces following equation:

$$\delta^{13}C_m \times C_m = \delta^{13}C_b \times C_b + \delta^{13}C_s \times C_s \tag{3}$$

OR,

$$\delta^{13}C_m = C_b \times (\delta^{13}C_b - \delta^{13}C_s) \times (1/C_m) + \delta^{13}C_s \tag{4}$$

$\delta^{13}C_m$, $\delta^{13}C_b$ and $\delta^{13}C_s$ are $\delta^{13}C$ ratios in mixture, background and added source component, respectively. Thus, to separate the source component from the background, a regression between measured $\delta^{13}C_m$ and ($1/C_m$) by CCIA is performed and slope (S) of the regression line was used to derive $\delta^{13}C_s$ i.e., CO_2 added from the source (from the OC-EC analyzer here).

$$C_b \times (\delta^{13}C_b - \delta^{13}C_s) = S \Rightarrow \delta^{13}C_s = \left(\delta^{13}C_b - \frac{S}{C_b} \right) \qquad (5)$$

Thermographs from OC-EC analysis show two distinct peaks of OC and EC fractions (in supplementary, Fig. S5). These peaks appear when the most abundant carbonaceous components are combusted and oxidized forming CO_2 exiting the OC-EC analyzer. Other times, CO_2 concentrations remained close to the background. Each peak lasted for ~1 to 1.5 minutes duration (depending upon the carbon load and vapor pressure of the organic compounds). The acquired data (1 s resolution) by CCIA was smoothened using 5 s integration to reduce noise in the measurement. NIOSH thermogram was modified to run for 180 s at starting ~34°C temperature (i.e., before ramping to higher temperature for sample combustion), instead of default 10 s. The middle 60 s of initial 180 s was averaged to estimate background CO_2 concentration (Fig. S5). This was done to estimate the sample specific background concentration (C_b) accurately which ensured no contamination of sample combusted produced CO_2. Any slight drift in CO_2 measurement by CCIA was also taken care of with this approach. The acquired CCIA data for OC peak with CO_2 values above C_b + standard deviation (which ensured non-inclusion of excessive number of background values in keeling curve) and corresponding isotope ratio values were used for keeling curve slope derivation. A robust weighted linear fitting to keeling plot was performed using matlab *robustfit* function to obtain slope accurately. The standard error in the slope, error in background concentration and norm of residual (Table S2) were used as variables to understand and quantify error in the isotopic ratio estimation as described in supplementary section S2. Error in slope should not exceed C_b values to contain below 1.0‰ error in isotopic ratio (Section S2-I). Operating CCIA at lower than 1300 ppm CO_2 concentration will incur below 1.0‰ error (Section S2-II). In the current practice, total time for each sample analysis is ~1 hour (~50 min for producing correction curve, ~10 min for analysis).

NIST standard sample (Li_2CO_3) used in this study contained only carbonate carbon thus data obtained from this peak was used to obtain the slope. This approach was applied to 5 Li_2CO_3 samples. Keeling approach produced accurate $\delta^{13}C$ ratio of NIST standard value with better than 1‰ precision (Table S1). Fig. 5(a) shows a representative Keeling plot of these 5 samples and slopes of such plots were used to derive the isotopic ratios (different samples produced almost same slopes for NIST standard) (Table S1). For example, slope of Fig. 5(a) (13108.21) will produce ~–46.74‰ (i.e., –20.8–13108/505.41 = ~46.74‰) using Eq. (5) (Table S1). The value –20.8‰ is the $\delta^{13}C$ of the reference gas.

This offline technique was applied to 10 ambient PM samples and an equal number of diesel exhaust PM samples. 5 replicate of ambient and diesel samples were also analyzed for ratio estimation. The OC isotope ratio of ambient and diesel replicates (following the same procedure as described for NIST standard), yielded almost same values with precision again better than 1.0‰ for both types of samples

(Table S1). The derived ratio values of OC for ambient and diesel exhaust aerosols (10 different samples) produced comparable results of $\delta^{13}C$ ratio (–27.9 to –22.7 and –26.2 to –22.9‰, respectively) with other studies (Widory, 2006; Cao *et al.*, 2011; Pavuluri *et al.*, 2011; Fu *et al.*, 2012; Kawashima and Haneishi, 2012; Mašalaitė *et al.*, 2012, Shakya *et al.*, 2012; Mkoma *et al.*, 2013; Kundu and Kawamura, 2014). Table 1 shows the measured isotopic values for aerosols of different origin. A representative Keeling plot for OC of ambient and diesel samples are also shown in Figs. 5(b) and 5(c) (slope of different samples was different for real samples) and $\delta^{13}C$ values for these are ~–27.90‰ and –24.90‰ respectively. The reported OC stable carbon isotopic ratios are well within the range of reported values in literature. There is no discernible difference of the ranges between ambient PM and engine exhaust PM samples, possibly due to the dominant vehicle emission impact on the collected roadside samples, and the mixture with the fossil fuel diesel samples.

The accuracy of slope from Keeling plot depends upon the shape of OC peak and OC mass. For example, narrower and steeper peak produce less number of data points (as is the case with diesel samples) and filter samples having organic carbon mass of 20 µg and above produce good number of data points for keeling curve slope derivation. Thus, for better derivation and accuracy, at least 20 µg of carbon in OC-EC analyzer is required for isotope ratio measurement and more is better because peak width and height will produce more number of data points for Keeling curve regression with improved accuracy. A slight drift in CCIA measurement during filter analysis may incur error in derivation of slope. Such drift is monitored using changes in ratio measurement of sample being analyzed from previous analyzed samples during background CO_2 measurement. If it is considerable different than previous analysis, sample is rejected. Thus, we recommend 3–5 replicates of sample analysis and select best ones having almost negligible drift. Other minor limitations are described in details in section S2. Typical seasonal average concentration of organic carbon in urban atmosphere is ~10–25 µg m^{-3} (Gu *et al.*, 2010) and three to four hours sampling at standard flow rate of 8 lpm will yield ~20–50 µg organic carbon, enough for the analysis of carbon isotopic composition by the developed method.

CONCLUSION

This study presented an experimental investigation to integrate Organic Carbon-Elemental Carbon (OC-EC) analyzer and Carbon Dioxide Isotope Analyzer (CCIA) for stable isotopic measurement of atmospheric carbonaceous particulate matter and theoretical analysis on the sources of measurement uncertainty. The method was successfully validated with NIST standards (Lithium Carbonate) of known isotopic composition. The approach requires correction of drift in $\delta^{13}C$ and CO_2 due to varying CO_2 and control of water vapor with a novel humidity stabilizer. Measurement on ambient aerosols and diesel exhaust aerosols also produced reasonable results in good agreement with literature values. This study demonstrates the utility of this tandem operation
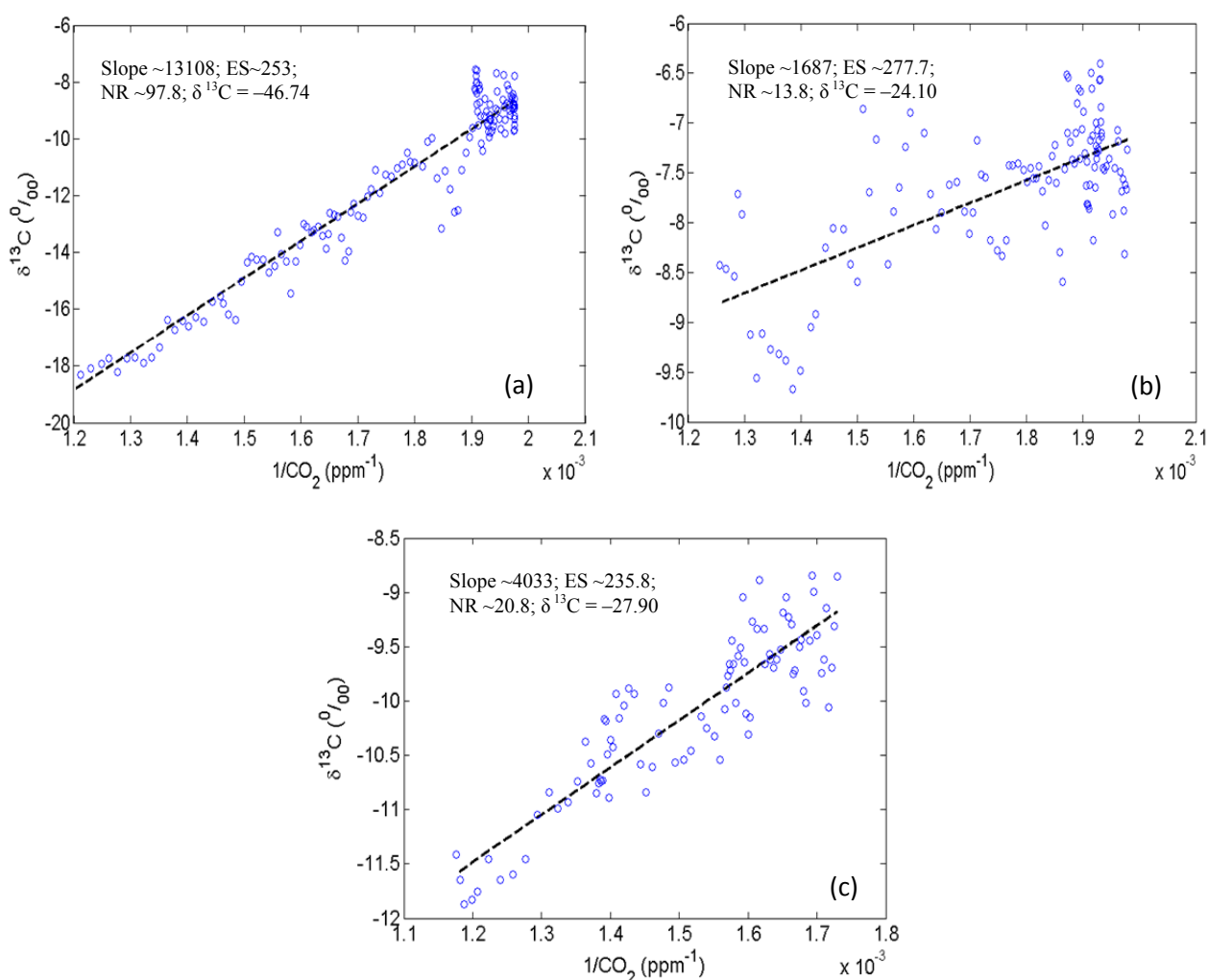
Fig. 5. Keeling plot for samples a). National Institute of Standards and Technology (NIST) standard; b) Diesel exhaust sample c) Ambient aerosol. ES and NR are error in slope and norm of residual, respectively.

Table 1. Typical values of stable isotopic ratio (in ‰) of aerosols from different origins.

Data source	Brief Description	$\delta^{13}C$ (OC)
This study	Ambient aerosol	–27.9 to –22.7
This study	Diesel exhaust	–26.2 to –22.9
Cao *et al.*, 2011	Ambient aerosols from Chinese cities	–26.6 to –23.1
Gustafsson *et al.*, 2009	Ambient aerosol	–24.2 to –20.9
Huang *et al.*, 2006	Ambient aerosol	–27.6 to –26.9
Huang *et al.*, 2006	Inside Tunnel	–27.0 to –25.4

for carbon isotopic measurement of atmospheric particles with better than 1.0‰ precision as an attractive alternative of conventional Isotopic Ratio Mass Spectrometer (IR-MS).

SUPPLEMENTARY MATERIALS

Supplementary data associated with this article can be found in the online version at http://www.aaqr.org.

REFERENCES

Adler, G., Flores, J. M., Abo Riziq, A., Borrmann, S. and Rudich, Y. (2011). Chemical, physical, and optical evolution of biomass burning aerosols: A case study. *Atmos. Chem. Phys.* 11: 1491–1503.

Alier, M., van Drooge, B. L., Dall'Osto, M., Querol, X., Grimalt, J.O. and Tauler, R. (2013). Source apportionment of submicron organic aerosol at an urban background and a road site in Barcelona (Spain) during SAPUSS. *Atmos. Chem. Phys.* 13: 10353–10371.

Birch, M.E. and Cary, R.A. (1996). Elemental carbon-based method for monitoring occupational exposures to particulate diesel exhaust. *Aerosol Sci. Technol.* 25: 221–241.

Cachier, H., Bremond, M.P. and Buat-Menard, P. (1989). Thermal separation of soot carbon. *Aerosol Sci. Technol.* 10: 358–364.

Cao, J.J., Lee, S.C., Ho, K.F., Zou, S.C., Fung, K., Li, Y., Watson, J.G. and Chow, J.C. (2004). Spatial and seasonal variations of atmospheric organic carbon and elemental carbon in Pearl River Delta Region, China. *Atmos. Environ.* 38: 4447–4456.

Cao, J.J., Chow, J.C., Tao, J., Lee, S.C., Watson, J.G., Ho, K.F., Wang, G.H., Zhu, C.S. and Han, Y.M. (2011). Stable carbon isotopes in aerosols from Chinese cities: Influence of fossil fuels. *Atmos. Environ.* 45: 1359–1363.

Cao, J.J., Zhu, C.S., Tie, X.X., Geng, F.H., Xu, H.M., Ho, S.S.H., Wang, G.H., Han, Y.M. and Ho, K.F. (2013). Characteristics and sources of carbonaceous aerosols from Shanghai, China. *Atmos. Chem. Phys.* 13: 803–817.

Ceburnis, D., Garbaras, A., Szidat, S., Rinaldi, M., Fahrni, S., Perron, N., Wacker, L., Leinert, S., Remeikis, V., Facchini, M.C., Prevot, A.S.H., Jennings, S.G., Ramonet, M. and O'Dowd, C.D. (2011). Quantification of the carbonaceous matter origin in submicron marine aerosol by ^{13}C and ^{14}C isotope analysis. *Atmos. Chem. Phys.* 11: 8593–8606.

Chow, J.C., Watson, J.G., Pritchett, L.C., Pierson, W.R., Frazier, C.A. and Purcell, R.G. (1993). The dri thermal/optical reflectance carbon analysis system: description, evaluation and applications in U.S. Air quality studies. *Atmos. Environ.* 27: 1185–1201.

Chow, J.C., Watson, J.G., Crow, D., Lowenthal, D.H. and Merrifield, T. (2001). Comparison of IMPROVE and NIOSH Carbon Measurements. *Aerosol Sci. Technol.* 34: 23–34.

Crippa, M., Canonaco, F., Lanz, V.A., Aijala, M., Allan, J.D., Carbone, S., Capes, G., Ceburnis, D., Dall'Osto, M., Day, D.A., DeCarlo, P.F., Ehn, M., Eriksson, A., Freney, E., Hildebrandt Ruiz, L., Hillamo, R., Jimenez, J.L., Junninen, H., Kiendler-Scharr, A., Kortelainen, A.M., Kulmala, M., Laaksonen, A., Mensah, A.A., Mohr, C., Nemitz, E., O'Dowd, C., Ovadnevaite, J., Pandis, S.N., Petaja, T., Poulain, L., Saarikoski, S., Sellegri, K., Swietlicki, E., Tiitta, P., Worsnop, D.R., Baltensperger, U. and Prevot, A.S.H. (2014). Organic aerosol components derived from 25 AMS data sets across Europe using a consistent ME-2 based source apportionment approach.

Atmos. Chem. Phys. 14: 6159–6176.

Croize, L., Mondelain, D., Camy-Peyret, C., Janssen, C., Lopez, M., Delmotte, M. and Schmidt, M. (2010). Isotopic composition and concentration measurements of atmospheric CO_2 with a diode laser making use of correlations between non-equivalent absorption cells. *Appl. Phys. B* 101: 411–421.

Ehn, M., Thornton, J.A., Kleist, E., Sipila, M., Junninen, H., Pullinen, I., Springer, M., Rubach, F., Tillmann, R., Lee, B., Lopez-Hilfiker, F., Andres, S., Acir, I.H., Rissanen, M., Jokinen, T., Schobesberger, S., Kangasluoma, J., Kontkanen, J., Nieminen, T., Kurten, T., Nielsen, L.B., Jorgensen, S., Kjaergaard, H.G., Canagaratna, M., Maso, M.D., Berndt, T., Petaja, T., Wahner, A., Kerminen, V.M., Kulmala, M., Worsnop, D.R., Wildt, J. and Mentel, T.F. (2014). A large source of low-volatility secondary organic aerosol. *Nature* 506: 476–479.

Fisseha, R., Saurer, M., Jäggi, M., Szidat, S., Siegwolf, R. T.W. and Baltensperger, U. (2006). Determination of stable carbon isotopes of organic acids and carbonaceous aerosols in the atmosphere. *Rapid Commun. Mass Spectrom.* 20: 2343–2347.

Fu, P.Q., Kawamura, K., Chen, J., Li, J., Sun, Y.L., Liu, Y., Tachibana, E., Aggarwal, S.G., Okuzawa, K., Tanimoto, H., Kanaya, Y. and Wang, Z.F. (2012). Diurnal variations of organic molecular tracers and stable carbon isotopic composition in atmospheric aerosols over Mt. Tai in the North China Plain: an influence of biomass burning. *Atmos. Chem. Phys.* 12: 8359–8375.

Gianfrani, L., Gabrysch, M., Corsi, C. and De Natale, P. (1997). Detection of H_2O and CO_2 with distributed feedback diode lasers: measurement of broadening coefficients and assessment of the accuracy levels for volcanic monitoring. *Appl. Opt.* 36: 9481–9486.

Gilardoni, S., Vignati, E., Marmer, E., Cavalli, F., Belis, C., Gianelle, V., Loureiro, A. and Artaxo, P. (2011). Sources of carbonaceous aerosol in the Amazon basin. *Atmos. Chem. Phys.* 11: 2747–2764.

Gu, J., Bai, Z., Liu, A., Wu, L., Xie, Y., Li, W., Dong, H. and Zhang, X. (2010). Characterization of Atmospheric Organic Carbon and Element Carbon of $PM_{2.5}$ and PM_{10} at Tianjin, China *Aerosol Air Qual. Res*. 10: 167–176.

Guillon, S. and Agrinier, E.P.P. (2012). Using a laser-based CO_2 carbon isotope analyser to investigate gas transfer in geological media. *Appl. Phys. B* 107: 449–457.

Gustafsson, O., Krusa, M., Zencak, Z., Sheesley, R.J., Granat, L., Engstrom, E., Praveen, P.S., Rao, P.S.P., Leck, C. and Rodhe, H. (2009). Brown clouds over south Asia: Biomasss or fossil fuel combustion? *Science* 323: 495–498.

Heo, J., Dulger, M., Olson, M.R., McGinnis, J.E., Shelton, B.R., Matsunaga, A., Sioutas, C. and Schauer, J.J. (2013). Source apportionments of $PM_{2.5}$ organic carbon using molecular marker Positive Matrix Factorization and comparison of results from different receptor models. *Atmos. Environ.* 73: 51–61.

Herriott, D.R. and Schulte, H.J. (1965). Folded Optical Delay Lines. *Appl. Opt.* 4: 883–889.

Herriott, D., Kogelnik, H. and Kompfner, R. (1964). Off-axis Paths in spherical mirror interferometers. *Appl. Opt.*

3: 523–526.

Huang, L., Brook, J.R., Zhang, W., Li, S.M., Graham, L., Ernst, D., Chivulescu, A. and Lu, G. (2006). Stable isotope measurements of carbon fractions (OC/EC) in airborne particulate: A new dimension for source characterization and apportionment. *Atmos. Environ.* 40: 2690–2705.

Irei, S., Takami, A., Hayashi, M., Sadanaga, Y., Hara, K., Kaneyasu, N., Sato, K., Arakaki, T., Hatakeyama, S., Bandow, H., Hikida, T. and Shimono, A. (2014). Transboundary secondary organic aerosol in Western Japan indicated by the $\delta^{13}C$ of water-soluble organic carbon and the *m/z* 44 signal in organic aerosol mass spectra. *Environ. Sci. Technol.* 48: 6273–6281.

Jimenez, J.L., Canagaratna, M.R., Donahue, N.M., Prevot, A.S.H., Zhang, Q., Kroll, J.H., DeCarlo, P.F., Allan, J.D., Coe, H., Ng, N.L., Aiken, A.C., Docherty, K.S., Ulbrich, I.M., Grieshop, A.P., Robinson, A.L., Duplissy, J., Smith, J.D., Wilson, K.R., Lanz, V.A., Hueglin, C., Sun, Y.L., Tian, J., Laaksonen, A., Raatikainen, T., Rautiainen, J., Vaattovaara, P., Ehn, M., Kulmala, M., Tomlinson, J.M., Collins, D.R., Cubison, M.J.E, Dunlea, J., Huffman, J.A., Onasch, T.B., Alfarra, M.R., Williams, P.I., Bower, K., Kondo, Y., Schneider, J., Drewnick, F., Borrmann, S., Weimer, S., Demerjian, K., Salcedo, D., Cottrell, L., Griffin, R., Takami, A., Miyoshi, T., Hatakeyama, S., Shimono, A., Sun, J.Y., Zhang, Y.M., Dzepina, K., Kimmel, J.R., Sueper, D., Jayne, J.T., Herndon, S.C., Trimborn, A.M., Williams, L.R., Wood, E.C., Middlebrook, A.M., Kolb, C.E., Baltensperger, U. and Worsnop, D.R. (2009). Evolution of organic aerosols in the atmosphere. *Science* 326: 1525–1529.

Kawashima, H. and Haneishi, Y. (2012). Effects of combustion emissions from the Eurasian continent in winter on seasonal $\delta^{13}C$ of elemental carbon in aerosols in Japan. *Atmos. Environ.* 46: 568–579.

Ke, L., Liu, W., Wang, Y., Russell, A.G., Edgerton, E.S. and Zheng, M. (2008). Comparison of $PM_{2.5}$ source apportionment using positive matrix factorization and molecular marker-based chemical mass balance. *Sci. Total Environ.* 394: 290–302.

Kirillova, E.N., Andersson, A., Tiwari, S., Srivastava, A.K., Bisht, D.S. and Gustafsson, Ö. (2014). Water-soluble organic carbon aerosols during a full New Delhi winter: Isotope-based source apportionment and optical properties. *J. Geophys. Res.* 119: 3476–3485.

Kundu, S. and Kawamura, K. (2014). Seasonal variations of stable carbon isotopic composition of bulk aerosol carbon from Gosan site, Jeju Island in the East China Sea. *Atmos. Environ.* 94: 316–322.

Lammel, G., Novak, J., Landlova, L., Dvorska, A., Klanova, J., Cupr, P., Kohoutek, J., Reimer, E. and Skrdlikova, L. (2010). Sources and distributions of polycyclic aromatic hydrocarbons and toxicity of polluted atmosphere aerosols. In *Urban Airborne Particulate Matter*, Zereini, F. and Wiseman, C.L.S. (Eds.), Environmental Science and Engineering, Springer Berlin Heidelberg.

Liu, J., Li, J., Zhang, Y., Liu, D., Ding, P., Shen, C., Shen, K., He, Q., Ding, X., Wang, X., Chen, D., Szidat, S. and Zhang, G. (2014). Source apportionment using radiocarbon

and organic tracers for $PM_{2.5}$ Carbonaceous aerosols in Guangzhou, South China: Contrasting local- and regional-scale haze events. *Environ. Sci. Technol.* 48: 12002–12011

Man, X.J., Cheung, C.S., Ning, Z. and Yung, K.F. (2015). Effect of waste cooking oil biodiesel on the properties of particulate from a diesel engine. *Aerosol Sci. Technol.* 49: 199–209.

Mašalaitė, A., Garbaras, A. and Remeikis, V. (2012). Stable isotopes in environmental investigations. *Lith. J. Phys.* 52: 261–268.

Masalaite, A., Remeikis, V., Garbaras, A., Dudoitis, V., Ulevicius, V. and Ceburnis, D. (2015). Elucidating carbonaceous aerosol sources by the stable carbon $\delta^{13}C_{TC}$ ratio in size segregated particles. *Atmos. Res.* 158–159: 1–12

McAlexander, I., Rau, G. H., Liem, J., Owano, T., Fellers, R., Baer, D. and Gupta, M. (2011). Deployment of a carbon isotope ratiometer for the monitoring of CO_2 sequestration leakage. *Anal. Chem.* 83: 6223–6229.

Miyazaki, Y., Fu, P.Q., Kawamura, K., Mizoguchi, Y. and Yamanoi, K. (2012). Seasonal variations of stable carbon isotopic composition and biogenic tracer compounds of water-soluble organic aerosols in a deciduous forest. *Atmos. Chem. Phys.* 12: 1367–1376.

Mkoma, S.L., Kawamura, K., Tachibana, E. and Fu, P. (2013). Stable carbon and nitrogen isotopic compositions of tropical atmospheric aerosols: sources and contribution from burning of C_3 and C_4 plants to organic aerosols. *Tellus Ser. B* 66: 1–14.

Pataki, D.E., Ehleringer, J.R., Flanagan, L.B., Yakir, D., Bowling, D.R., Still, C.J., Buchmann, N., Kaplan, J.O. and Berry, J.A. (2003). The application and interpretation of Keeling plots in terrestrial carbon cycle research. *Global Biogeochem. Cycles* 17: 1022.

Pavuluri, C.M., Kawamura, K., Swaminathan, T. and Tachibana, E. (2011). Stable carbon isotopic compositions of total carbon, dicarboxylic acids and glyoxylic acid in the tropical Indian aerosols: Implications for sources and photochemical processing of organic aerosols. *J. Geophys. Res.* 116: D18307.

Ramanathan, V., Chung, C., Kim, D., Bettge, T., Buja, L., Kiehl, J.T., Washington, W.M., Fu, Q., Sikka, D.R. and Wild, M. (2005). Atmospheric brown clouds: Impacts on South Asian climate and hydrological cycle. *Proc. Natl. Acad. Sci. U.S.A.* 102: 5326–5333.

Shakya, K.M., Place, P.F., Griffin, R.J. and Talbot, R.W. (2012). Carbonaceous content and water-soluble organic functionality of atmospheric aerosols at a semi-rural New England location. *J. Geophys. Res.* 117: D03301.

Tie, X., Wu, D. and Brasseur, G. (2009). Lung cancer mortality and exposure to atmospheric aerosol particles in Guangzhou, China. *Atmos. Environ.* 43: 2375–2377.

Wang, M., Xu, B., Cao, J., Tie, X., Wang, H., Zhang, R., Qian, Y., Rasch, P.J., Zhao, S., Wu, G., Zhao, H., Joswiak, D.R., Li, J. and Xie, Y. (2014). Carbonaceous aerosols recorded in a Southeastern Tibetan glacier: variations, sources and radiative forcing. *Atmos. Chem. Phys.* 15: 1191–1204.

Werle, P., Mucke, R. and Slemr, F. (1993). The limits of

signal averaging in atmospheric trace-gas monitoring by tunable diode-laser absorption spectroscopy (TDLAS). *Appl. Phys. B* 57: 131–139.

Werle, P. (2011). Accuracy and precision of laser spectrometers for trace gas sensing in the presence of optical fringes and atmospheric turbulence. *Appl. Phys. B* 102: 313–329.

Widory, D. (2006). Combustibles, fuels and their combustion products: A view through carbon isotopes. *Combust. Theor. Model.* 10: 831–841.

Wilson, K.L. and Birks, J.W. (2006). Mechanism and elimination of a water vapor interference in the measurement of ozone by UV absorbance. *Environ. Sci. Technol.* 40: 6361–6367.

Xu, H., Wang, Y., Wen, T., Yang, Y. and Zhao, Y. (2009). Characteristics and source apportionment of atmospheric aerosols at the summit of Mount Tai during summertime. *Atmos. Chem. Phys. Discuss.* 9: 16361–16379.

Yang, F., Kaul, D., Wong, K. C., Westerdahl, D., Sun, L., Ho, K.F., Tian, L., Brimblecombe, P. and Ning, Z. (2014). Heterogeneity of passenger exposure to air pollutants in public transport microenvironments. *Atmos. Environ.* 109: 42–51.

Yang, H. and Yu, J.Z. (2002). Uncertainties in charring correction in the analysis of elemental and organic carbon in atmospheric particles by thermal/optical methods. *Environ. Sci. Technol.* 36: 5199–5204.

Zhang, Q., Jimenez, J.L., Canagaratna, M.R., Allan, J.D., Coe, H., Ulbrich, I., Alfarra, M.R., Takami, A., Middlebrook, A.M., Sun, Y.L., Dzepina, K., Dunlea, E., Docherty, K., DeCarlo, P.F., Salcedo, D., Onasch, T., Jayne, J.T., Miyoshi, T., Shimono, A., Hatakeyama, S., Takegawa, N., Kondo, Y., Schneider, J., Drewnick, F., Borrmann, S., Weimer, S., Demerjian, K., Williams, P., Bower, K., Bahreini, R., Cottrell, L., Griffin, R.J., Rautiainen, J., Sun, J.Y., Zhang, Y.M. and Worsnop, D.R. (2007). Ubiquity and dominance of oxygenated species in organic aerosols in anthropogenically-influenced Northern Hemisphere midlatitudes. *Geophys. Res. Lett.* 34: L13801.

Zhang, Y.L., Li, J., Zhang, G., Zotter, P., Huang, R.J., Tang, J.H., Wacker, L., Prevot, A.S.H. and Szidat, S. (2014). Radiocarbon-based source apportionment of carbonaceous aerosols at a regional background site on Hainan Island, South China. *Environ. Sci. Technol.* 48: 2651–2659.

Zhou, J.H., Cheung, C.S. and Leung, C.W. (2014). Combustion, performance, regulated and unregulated emissions of a diesel engine with hydrogen addition. *Appl. Energy* 126: 1–12.